Early stage of plastic deformation in thin films undergoing electromigration

B. C. Valek
Department Materials Science and Engineering, Stanford University, Stanford, California 94305

N. Tamura[a)]
Advanced Light Source, 1 Cyclotron Road, Berkeley, California 94720

R. Spolenak
Max-Planck-Institut für Metallforschung, Heisenbergstrasse3, D-70569 Stuttgart, Germany

W. A. Caldwell, A. A. MacDowell, R. S. Celestre, and H. A. Padmore
Advanced Light Source, 1 Cyclotron Road, Berkeley, California 94720

J. C. Bravman
Department Materials Science and Engineering, Stanford University, Stanford, California 94305

B. W. Batterman
Advanced Light Source, 1 Cyclotron Road, Berkeley, California 94720 and SSRL/SLAC, Stanford University, 2575 Sand Hill Road, Menlo Park, California 94025

W. D. Nix
Department Materials Science and Engineering, Stanford University, Stanford, California 94305

J. R. Patel
Advanced Light Source, 1 Cyclotron Road, Berkeley, California 94720 and Department Materials Science and Engineering, Stanford University, California 94305

(Received 4 April 2003; accepted 24 June 2003)

Electromigration occurs when a high current density drives atomic motion from the cathode to the anode end of a conductor, such as a metal interconnect line in an integrated circuit. While electromigration eventually causes macroscopic damage, in the form of voids and hillocks, the earliest stage of the process when the stress in individual micron-sized grains is still building up is largely unexplored. Using synchrotron-based x-ray microdiffraction during an *in-situ* electromigration experiment, we have discovered an early prefailure mode of plastic deformation involving preferential dislocation generation and motion and the formation of a subgrain structure within individual grains of a passivated Al (Cu) interconnect. This behavior occurs long before macroscopic damage (hillocks and voids) is observed. © *2003 American Institute of Physics.* [DOI: 10.1063/1.1600843]

I. INTRODUCTION

Metal thin films[1] patterned into micron-scale structures called interconnects comprise the communication network of all integrated circuits. These structures, which carry electrical signals between the millions of individual transistors on a modern integrated circuit, can be deleteriously affected by a phenomenon called electromigration[1,2] (EM). This arises when the electrical current densities in the interconnects become large enough to significantly influence the diffusion of atoms, inducing voids and hillocks to form under certain circumstances and eventually resulting in the possible failure of the device. Experiments have shown that the microstructure of these interconnects significantly affects this process.[3–6] It is also known that the development of a stress gradient in the interconnect, which necessarily attends electromigration, can impede or completely halt the process.[7] While plastic deformation is expected to occur during electromigration when the stress gets high enough, quantitative information on plasticity during *in-situ* electromigration tests is difficult to obtain, because of the size of the structures and of the local nature of the phenomenon. Recent work by other groups[8,9] using x-ray microdiffraction (1–10 μm beam size) addressed lattice parameter measurements but not the question of EM-induced plasticity. Scanning electron microscopy, transmission electron microscopy, and x-ray microscopy studies concentrated mainly on the evolution of the most visible outcomes of plastic deformation, i.e., the creation of voids and hillocks.[10–12] Using white beam x-ray microdiffraction,[13–15] we have recently discovered that plastic deformation starts at a very early stage during the electromigration process, well before any visible damage develops in the conducting line.[16] In this article we report a quantitative analysis of this early stage of EM-induced plasticity in individual grains of a buried (passivated) Al (Cu) single interconnect line.

Quantitative x-ray investigations of matter on a micron scale have only recently become possible with the advent of third generation synchrotron sources and development of suitable white and monochromatic crystal optics.[17] Because of its achromaticity, a pair of orthogonal elliptical mirrors (Kirkpatrick–Baez configuration) is the best way to produce an intense high quality white light focus[18–21] The present

a)Electronic mail: ntamura@lbl.gov

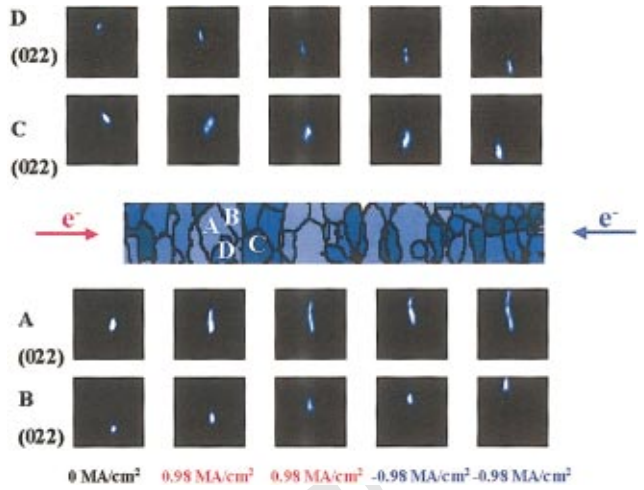

FIG. 1. (Color) Grain orientation map obtained by white beam scanning x-ray microdiffraction (center) and evolution of the (022) peak shape for grains labeled A, B, C, and D. Peak shift, streaking, and splitting are observed during the course of the EM experiment.

x-ray microdiffraction measurements have been carried out on the 7.3.3. bending magnet beamline at the Advanced Light Source ■, ■, where Kirkpatrick–Baez focusing mirrors are produced by controlled bending of specially contoured perfectly flat substrates.[20]

II. EXPERIMENT

The test interconnect lines were fabricated from sputtered Al (0.5 wt % Cu) film on an oxidized silicon substrate. Two shunt layers of Ti 450 Å at the bottom and 100 Å at the top sandwich the Al (Cu) line The lithographically patterned lines were passivated (buried) under an overgrown SiO_2 oxide layer and received a furnace homogenizing treatment at 400 °C for 30 min. Measurements were made on 4.1 μm wide, 0.75 μm thick, and 30 μm long lines. Using a white x-ray microbeam of size $0.8\times0.7\,\mu$m, grain orientations were established by collecting Laue patterns with a large area x-ray charge coupled device (CCD) detector. Custom software[15] was used to index the white-beam Laue spots even in the case where multiple grains were illuminated. The sample was mounted on a scanning stage and the test lines were scanned in 0.5 μm intervals to obtain Laue diffraction images at each step.

III. RESULTS AND DISCUSSION

In the center of Fig. 1 we show a grain orientation map of a 30 μm long line determined from the scans described above.[15,21] We focus attention on the four grains marked A, B, C, and D. The (022) reflections of these grains are shown as a function of applied current density and current direction in an accelerated electromigration test at a temperature of 205 °C. With no current applied the spots are narrow in width and have the usual shape observed in as-deposited annealed films. Once the current is applied in the direction shown, the spots both streak and rotate from their original position, while silicon Laue spots originating from the substrate remain fixed. The streaking and rotation observed at a constant current density grow more pronounced with time. When the current is reversed we observe, in the example shown here, that streaking and rotation of the spots continues and neither a decrease in streaking nor reversal in rotation is observed. We also note that in many cases the streak intensity is not uniform and individual spots can be seen within the streak. Control measurements made in parallel and at the same temperature on similar interconnect lines with no current applied confirm that the above observed peak streaking and rotations are solely induced by the applied current flow.

The observations in Fig. 1 are remarkable in several ways. Early experiments[7] and simulations[22,23] have proposed the evolution of a linear gradient in hydrostatic stress along the conducting line, induced by the current driven mass flow. This can be correlated with a gradient in vacancy concentration. Local equilibrium between stress and vacancy concentration, is usually assumed. In the transient state of the stress build-up, the atoms transported have to be incorporated or emitted from atomic sinks or sources, such as dislocations or grain boundaries present in the thin film. Interfaces such as Al/Ti also play a role. Assuming that local shear deformation occurs in the grain, Laue spot broadening could be expected. However, it is not obvious whether the individual dislocations or grain boundaries introduced should be oriented parallel or perpendicular to the conducting line. The observations in Fig. 1 now reveal that the spots are streaked across the line indicating that the individual grains are curved or bent transverse to the direction of electron flow. Bending implies that in individual grains the distribution of dislocations is predominantly of one sign and lies parallel to the direction of current flow.

The streak data can be used to quantitatively estimate the geometrically necessary dislocation (GND) density required for apparent bending of the grains. For grain A, after allowing a current of 0.98 MA/cm^2 to flow for 20 h at 205 °C and then reversing the current direction for a further 10 h the curvature angle is 1.23° measured from the length of the streak on the CCD and the calibrated detector to sample distance. The grain width is 2.5 μm from which a radius of curvature of $R=116\,\mu$m is derived. The Cahn–Nye[24,25] relation $\rho=(1/Rb)$ relates the radius of curvature R to the dislocation density ρ and to the component b of the Burgers vector on the neutral axis. For simplicity we assume that the active slip system is in the vicinity of 45°. For a fcc Al crystal, with $1/2\langle110\rangle$ Burgers vector, $|\mathbf{b}|=2.864$ Å. Using the above values we find the dislocation density in this grain $\rho=3\times10^9/\text{cm}^2$. This is a reasonable value for a plastically deformed Al crystal.[26] For the relevant dimensions of the crystal involved here, we note that a total of 55 dislocations of one sign are sufficient to accommodate the inferred plastic deformation.

It is also evident from Fig. 1 that the streak intensity, especially in the later stages of plastic deformation, is not uniform and breaks up into well-defined and resolvable spots. Details of the evolution of the streaking for the (022) reflection of grain A together with an intensity profile of the streak, are shown in Fig. 2(a). The splitting profile [Fig. 2(b)] shows clearly resolved peaks, which indicates that the individual crystal grain breaks up into segments with their own

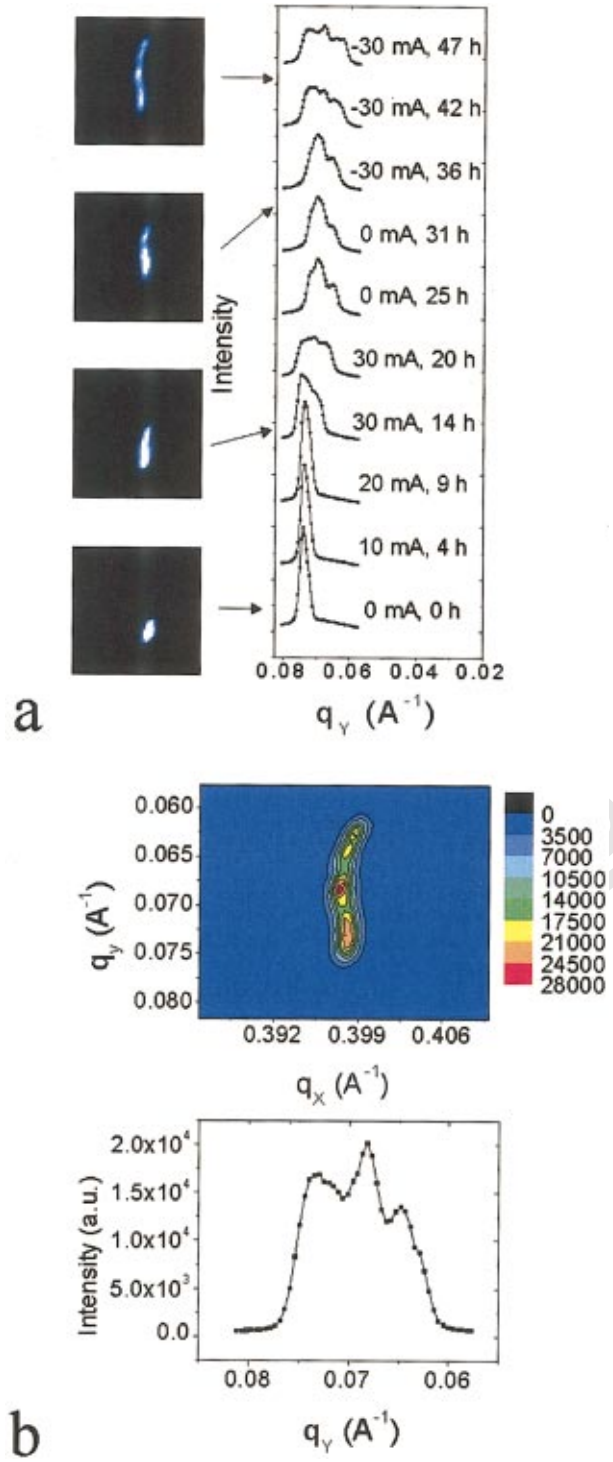

FIG. 2. (Color) (a) Evolution of the peak shape and profile of the (022) reflection for the grain labeled A in Fig. 1. (b) Detail of the peak shape and profile after 47 hours. The reflection has clearly split into three subpeaks indicating the formation of three slightly misoriented subgrains. *X* refers to the direction along the line while *Y* is the direction across the line.

well-defined orientation. The general phenomenon is known as polygonization and has been observed and measured in bulk crystals subject to pure bending.[27] In the polygonization process, the dislocations introduced during deformation climb to arrange themselves one above the other into a small-angle grain boundary separating subgrains. This vertical arrangement results in a significant reduction in elastic

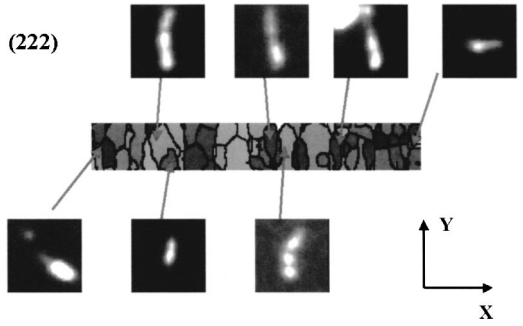

FIG. 3. (222) Peak profiles of different grains in the aluminum line after 47 hours of EM test. Most of the peak broadenings occur in the direction across the line, except at the very ends of the line, where it goes along the line.

energy because of the cancellation of the alternating tensile and compressive strain fields associated with edge dislocations. From the splitting of the streaks, the misorientation between adjacent blocks can be measured. Using the measured misorientation, the spacing between dislocations in the boundary can be derived using the Burgers relation for a small angle grain boundary $\theta=(|\mathbf{b}|/L)$. Here, θ is the measured misorientation angle, **b** is the Burgers vector, and L the spacing between dislocations in the boundary. For the measured angle between spots of $\theta=0.57°$ and for $\mathbf{b}=1/2\langle 110\rangle$ we obtain $L=288$ Å. For a film thickness of 0.75 μm this amounts to 26 dislocations in the boundary. For grain A in Fig. 2, the splitting of the Laue reflection into three different subpeaks implies that two small angle boundaries and three subgrains have been produced during the electromigration process. While the boundary dislocations represent a good fraction of the geometrically necessary dislocations (GND) produced, direct observations on bending deformation of macroscopic specimens show that the dislocation density in material deformed in bending is always higher[27] than the GND's. It is only after annealing, when the crystal polygonizes, that the total dislocation density approaches the GND density.

Figure 3 shows (222) diffraction streaks at chosen grains along the line after allowing a current of 0.98 MA/cm^2 to flow for 20 h at 205 °C and then reversing the current direction for a further 10 h. While deformation pervades the length of the line, its extent is highly variable and strongly dependent on grain size.

The large grain A in Fig. 1 shows both rotation and extensive streaking. However, the smaller grains marked B, C, and D rotate but show only moderate streaking which is to be expected since small grains are more resistant to plastic flow.[28,29] We have also observed this grain-size effect in several other electromigration experiments. The general direction of streaking away from the ends is transverse to the line for all grains. Some grains at both ends of the line where the current diverges at the buried contact vias below the line, show streaking along the line (Fig. 3).

To gain additional insight into these observations, we note that in Fig. 3, a few grains span the width of the line, while the preponderance of the line consists of either two or three grains across the line. As soon as the current is switched on atoms begin to move along the whole length of

the line. Our previous experimental observations[16] indicate that early in the transient stage of electromigration plastic deformation of the grains is greatest at the cathode end and decreases as we approach the anode end. For simplicity let us consider a single grain across the line at the cathode end. In this situation the Al/Ti interface or the grain boundaries normal to the electron flow are likely the main sources and sinks for point defects. Multiple grains will introduce another source and sink besides the surfaces, i.e., a grain boundary with components parallel to the direction of electron flow. Several studies have suggested that atomic flow due to electromigration preferentially occurs at defects and interfaces rather than in the crystal lattice.[30,31] Atomic migration along dislocation cores and grain boundaries is indeed many orders of magnitude faster than in bulk aluminum.[32] as the interfaces of the line are different on the sidewalls (Al/SiO_2), and at the top and the bottom (Al/Ti), the diffusivities of the associated diffusion paths are different as well. The observed Laue streaking indicating bending or curvature of grains starting at the cathode end is consistent with a preferential atomic motion at the Al/Ti interface. Let us first consider grain A which roughly spans the width of the line. If we assume that atomic motion primarily occurs at the Al/Ti interface a supersaturation of vacancies will rapidly build up at the top and bottom surfaces, and these vacancies will over time diffuse into the bulk of the grain as shown in schematically in Fig. 4(a). Some vacancy motion from the sidewalls and blocking grain boundaries cannot be ruled out. At the bottom interface the constraint from the substrate is quite rigid. However in the top half of the grain the constraint due to the more compliant dielectric is less severe and the tensile stresses introduced by the vacancy diffusion can be relaxed by plastic flow as illustrated in Fig. 4(b). Given the rigidity of the bottom interface the stress in the lower half of the grain will be larger than the upper resulting in dislocations being introduced from this surface along the active slip planes as indicated in Fig. 4(b). The concave bending is the response of the material to partially relieve this tensile stress. To account for the observed curvature also requires that the enclosing dielectric distort enough at 205 °C to accommodate a maximum strain of about 3×10^{-3}. It is also evident from the insets showing the Laue spots that the rotation of the streaks from the original spot position at time zero indicates an inward motion across the line demonstrating that the grain curvature is concave. During slip some polygonization will occur as observed in macroscopic experiments on bulk crystals.[27] This is illustrated schematically in Fig. 4(b) as dislocation walls normal to the slip lines.

For grains B and C where there are grain boundary components along the direction of electron flow vacancies generated or diffusing to this boundary will deplete material in the boundary this will tend to shrink the material in the upper halves of the two grains, since the bottom half is more rigidly constrained than the top. Material shrinkage in the upper half of the grain is most likely accomplished by a dislocation climb at the grain boundary and the eventual elimination of the extra half plane of dislocations with an edge component. The resulting rotation in addition to some streaking of the spots due to plastic bending of the grains is observed experimentally as seen in Fig. 1. The streaking is not as pronounced as observed in the larger grain A and is consistent with our earlier statement about the resistance of smaller grains to plastic flow. This situation is illustrated in Fig. 4(c) which shows a cross section of the two grains before plastic deformation but with an accumulation of vacancies in the vicinity of the grain boundary. Only the top halves of the two grains can relax since the bottom is rigidly constrained by the substrate. The resulting plastic bending and grain rotation that is a consequence of the depletion of material at the grain boundary is shown in Fig. 4(d). We also show an inset in Fig. 4(d) indicating the direction of the rotation of the Laue spots for grains B and C which again demonstrates the concave shape of the deformed grains.

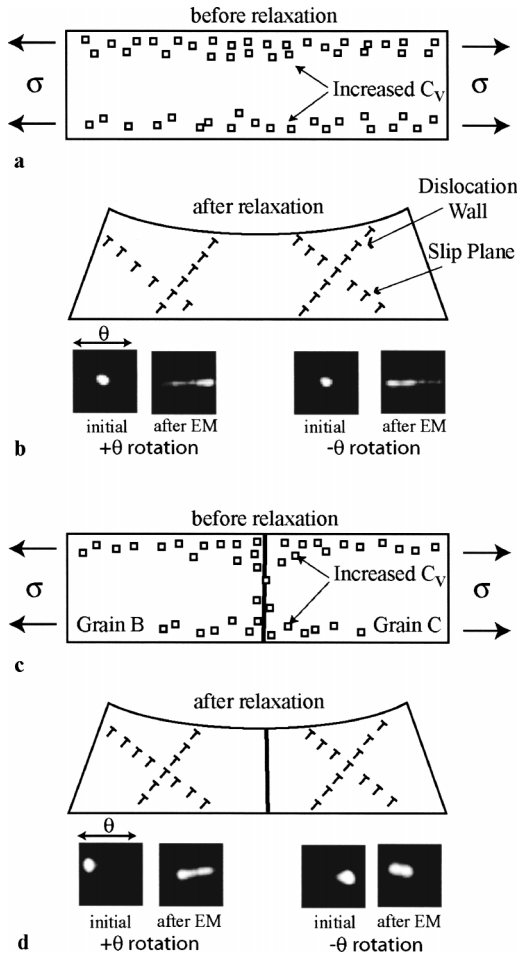

FIG. 4. (a) Schematic cross section of grain A illustrating the accumulation of vacancies diffusing in from the surfaces, (b) plastic deformation of the crystal in response to the stresses built up in the crystal. Some polygonization can also occur during slip as indicated schematically by the vertical lining up of dislocations. Insets show the rotation and streaking of Laue spots at the two ends of the grain, (c) schematic of a cross section of two grains with a boundary between them and the accumulation of vacancies in the vicinity of the grain boundary, and (d) plastic deformation of the grains showing excess dislocations of one sign to account for the concave shape after plastic flow. Inset shows Laue spot positions before and after EM.

The deficiency of atoms at the cathode end of the line, could result in the formation of voids at a later stage of electromigration. However at this stage in the process our post-electromigration Focused ion beam (FIB) cross sections do not show any voids or hillocks in the interconnect line.

What we have observed using x-ray microdiffraction is therefore a very early stage in the electromigration process where stresses get large enough to plastically distort grains but not enough to nucleate voids or form hillocks.

IV. SUMMARY

In summary, using white beam x-ray microdiffraction, we have observed an unexpected mode of an early stage of plastic deformation induced by electromigration, during an *in-situ* experiment on a passivated Al (Cu) conducting line. Individual grains deform in a manner that introduces dislocations and small angle grain boundaries in the direction of electron flow. From the streaking of the Laue reflections we obtain the radius of curvature of individual grains and calculate the number of dislocations necessary to account for the curvature. By measuring the splitting of the Laue streaks into spots we calculate the dislocation spacing in the small angle grain boundaries that form within individual grains. We have proposed a model for the deformation of individual grains that involves the flow of vacancies generated by electromigration mostly at interfaces into the bulk of individual grains resulting in stresses being built up that cause plastic flow. The consequences of these findings could be important to our understanding of the overall mechanics of EM-induced failure. For instance, this prefailure mode creates new interfaces for atomic diffusion in later stages of the electromigration process in the form of dislocations and subgrain boundaries parallel to the direction of the current. If dislocation climb is the main mechanism to form these sub-grain boundaries, the present observations may lead to new insights for predicting electromigration lifetimes.

ACKNOWLEDGMENTS

The Advanced Light Source is supported by the Director, Office of Science, Office of Basic Energy Sciences, Materials Sciences Division, of the U.S. Department of Energy under Contract No. DE-AC03-76SF00098 at Lawrence Berkeley National Laboratory. We also thank John Carruthers and Intel Corporation for encouragement and generous help towards instrumenting the Microdiffraction beamline. We are indebted to E. Arzt and A. Robinson for critical comments. SRC support for this project Task 945.001 and its extension to Cu interconnects, under a grant from Intel Corporation, is gratefully acknowledged.

[1] J. D. Plummer, M. D. Deal, and P. B. Griffin, *Silicon VLSI Technology Fundamentals, Practice and Modeling* (Prentice Hall, Upper Saddle River, NJ, 2000).
[2] H. B. Huntington and H. B. Grone, J. Phys. Chem. Solids **20**, 76 (1961).
[3] T. Marieb, P. Flinn, and J. C. Bravman, J. Appl. Phys. **78**, 1026 (1995).
[4] D. B. Knorr and K. P. Rodbell., J. Appl. Phys. **79**, 2409 (1996).
[5] O. Kraft and E. Arzt, Acta Mater. **46**, 3733 (1998).
[6] E. Arzt, O. Kraft, R. Spolenak, and Y. C. Joo, Z. Metallkd. **87**, 934 (1996).
[7] I. A. Blech and C. Herring, Appl. Phys. Lett. **29**, 131 (1976).
[8] P.-C. Wang, G. S. Cargill, I. C. Noyan, and C.-K. Hu, Appl. Phys. Lett. **72**, 1296 (1998).
[9] X. Zhang, H. Solak, F. Cerrina, B. Lai, Z. Cai, P. Ilinski, D. Legnini, and W. Rodrigues, Appl. Phys. Lett. **76**, 315 (2000).
[10] T. Marieb, P. Flinn, J. C. Bravman, D. Gardner, and M. Madden, J. Appl. Phys. **78**, 1026 (1995).
[11] W. C. Shih and A. L. Greer, J. Appl. Phys. **84**, 2551 (1998).
[12] G. Schneider, G. Denbeaux, E. H. Anderson, B. Bates, A. Pearson, M. A. Meyer, E. Zschech, D. Hambach, and E. A. Stach, Appl. Phys. Lett. **81**, 2535 (2002).
[13] J.-S. Chung and G. E. Ice, J. Appl. Phys. **86**, 5249 (1999).
[14] N. Tamura, R. S. Celestre, A. A. MacDowell, H. A. Padmore, R. Spolenak, B. C. Valek, N. Meier Chang, A. Manceau, and J. R. Patel, Rev. Sci. Instrum. **73**, 1369 (2002).
[15] N. Tamura, A. A. MacDowell, R. Spolenak, W. L. Brown, B. C. Valek, J. C. Bravman, R. S. Celestre, H. A. Padmore, B. W. Batterman, and J. R. Patel, J. Synchrotron Radiat. **10**, 137 (2003).
[16] B. C. Valek, J. C. Bravman, N. Tamura, A. A. MacDowell, R. S. Celestre, H. A. Padmore, R. Spolenak, W. L. Brown, B. W. Batterman, and J. R. Patel., Appl. Phys. Lett. **81**, 4168 (2002).
[17] G. E. Ice, X-Ray Spectrom. **26**, 315 (1997).
[18] H. A. Padmore, G. Ackerman, R. S. Celestre, C.-H. Chang, K. Franck, M. Howells, Z. Hussain, S. Irick, S. Locklin, A. A. MacDowell, J. R. Patel, A.-Y. Rah, T. R. Renner, and R. Sandler, Synchrotron Radiat. News **10.6**, 18 (1997).
[19] G. E. Ice, J.-S. Chung, J. Z. Tischler, A. Lunt, and L. Assoufid, Rev. Sci. Instrum. **71**, 2635 (2000).
[20] A. A. MacDowell, R. S. Celestre, N. Tamura, R. Spolenak, B. C. Valek, W. L. Brown, J. C. Bravman, H. A. Padmore, B. W. Batterman, and J. R. Patel, Nucl. Instrum. Methods Phys. Res. A **467–468**, 936 (2001).
[21] O. Hignette, G. Rostaing, P. Cloetens, A. Rommeveaux, W. Ludwig, and A. Freund, Proc. SPIE **4499**, 105 (2001).
[22] N. Tamura, A. A. MacDowell, R. S. Celestre, H. A. Padmore, B. Valek, J. C. Bravman, R. Spolenak, W. L. Brown, T. Marieb, H. Fujimoto, B. W. Batterman, and J. R. Patel, Appl. Phys. Lett. **80**, 3724 (2002).
[23] M. A. Korhonen, P. Børgesen, K.-N. Tu, and C.-Y. Li, J. Appl. Phys. **73**, 3790 (1993).
[24] R. W. Cahn, J. Inst. Met. **86**, 121 (1949).
[25] J. F. Nye, Acta Metall. **1**, 153 (1953).
[26] R. E. Reed-Hill., *Physical Metallurgy Principles* (PWS Publishers, Boston, 1973), pp. 268-277.
[27] J. R. Patel, J. Appl. Phys. **29**, 170 (1958).
[28] B. Von Blanckenhagen, P. Gumbsch, and E. Arzt, *Modelling & Simulation in Materials Science & Engineering*, Vol. 9 (IOP Publishing, UK, 2001), pp. 157–169.
[29] C. V. Thompson, J. Mater. Res. **8**, 237 (1993).
[30] J. A. Bohm, C. A. Volkert, R. Monig, T. J. Balk, and E. Arzt, J. Electron. Mater. **31**, 45 (2002).
[31] J. A. Nucci, A. Straub, E. Bischoff, E. Arzt, and C. A. Volkert, J. Mater. Res. **17**, 2727 (2002).
[32] A. P. Sutton and R. W. Balluffi, *Interfaces in Crystalline Materials* (Oxford University Press, New York, 1995), pp. 467-521.